

Efficient light coupling into in-plane semiconductor nanomembrane photonic devices utilizing a sub-wavelength grating coupler

Harish Subbaraman,^{1,3,*} Xiaochuan Xu,^{2,3} John Covey,² and Ray T. Chen²

¹*Omega Optics, Inc, 10306 Sausalito Dr, Austin, Texas 78759, USA*

²*Department of Electrical and Computer Engineering, The University of Texas at Austin, 10100 Burnet Rd, PRC/MER 160, Austin, Texas 78758, USA*

³*Joint first authors*

*harish.subbaraman@omegaoptics.com

Abstract: We report a subwavelength grating (SWG) coupler for coupling light efficiently into in-plane semiconductor nanomembrane photonic devices for the first time. The SWG coupler consists of a periodic array of rectangular trenches fabricated on a silicon nanomembrane (SiNM) transferred onto a glass substrate. At a wavelength of 1555.56 nm, the coupling efficiency of the fabricated 10 μm wide, 17.1 μm long SWG is 39.17% (−4.07 dB), with 1 dB and 3 dB bandwidths of 29 nm and 57 nm, respectively. Peak efficiency varies by 0.26 dB when measuring 5 fabricated grating pairs. Coupling efficiency can further be improved with an improved SiNM transfer process. Such high efficiency couplers allow for the successful realization of a plethora of hybrid photonic devices utilizing nanomembrane technology.

©2012 Optical Society of America

OCIS codes: (050.6624) Subwavelength structures; (050.2770) Gratings; (130.0130) Integrated optics; (130.1750) Components; (160.1245) Artificially engineered materials.

References and links

1. E. Menard, K. J. Lee, D.-Y. Khang, R. G. Nuzzo, and J. A. Rogers, "A printable form of silicon for high performance thin film transistors on plastic substrates," *Appl. Phys. Lett.* **84**(26), 5398–5400 (2004).
2. E. Menard, R. G. Nuzzo, and J. A. Rogers, "Bendable single crystal silicon thin film transistors formed by printing on plastic substrates," *Appl. Phys. Lett.* **86**(9), 093507 (2005).
3. F. Cavallo and M. G. Lagally, "Semiconductors turn soft: inorganic nanomembranes," *Soft Matter* **6**(3), 439–455 (2010).
4. M. M. Roberts, L. J. Klein, D. E. Savage, K. A. Slinker, M. Friesen, G. Celler, M. A. Eriksson, and M. G. Lagally, "Elastically relaxed free-standing strained-silicon nanomembranes," *Nat. Mater.* **5**(5), 388–393 (2006).
5. D. H. Kim, J. H. Ahn, W. M. Choi, H. S. Kim, T. H. Kim, J. Z. Song, Y. Y. Huang, Z. J. Liu, C. Lu, and J. A. Rogers, "Stretchable and foldable silicon integrated circuits," *Science* **320**(5875), 507–511 (2008).
6. M. A. Meitl, Z. T. Zhu, V. Kumar, K. J. Lee, X. Feng, Y. Y. Huang, I. Adesida, R. G. Nuzzo, and J. A. Rogers, "Transfer printing by kinetic control of adhesion to an elastomeric stamp," *Nat. Mater.* **5**(1), 33–38 (2006).
7. J. A. Rogers, M. G. Lagally, and R. G. Nuzzo, "Synthesis, assembly and applications of semiconductor nanomembranes," *Nature* **477**(7362), 45–53 (2011).
8. Y. Yang, Y. Hwang, H. A. Cho, J. H. Song, S. J. Park, J. A. Rogers, and H. C. Ko, "Arrays of Silicon Micro/Nanostructures Formed in Suspended Configurations for Deterministic Assembly Using Flat and Roller-Type Stamps," *Small* **7**(4), 484–491 (2011).
9. J.-H. Ahn, H.-S. Kim, K. J. Lee, Z. Zhu, E. Menard, R. G. Nuzzo, and J. A. Rogers, "High-Speed Mechanically Flexible Single-Crystal Silicon Thin-Film Transistors on Plastic Substrates," *IEEE Electron Device Lett.* **27**(6), 460–462 (2006).
10. D.-H. Kim, J.-H. Ahn, H.-S. Kim, K. J. Lee, T.-H. Kim, C.-J. Yu, R. G. Nuzzo, and J. A. Rogers, "Complementary Logic Gates and Ring Oscillators on Plastic Substrates by Use of Printed Ribbons of Single-Crystalline Silicon," *IEEE Electron Device Lett.* **29**(1), 73–76 (2008).
11. H. Pang, H.-C. Yuan, M. G. Lagally, G. K. Celler, and Z. Ma, "Flexible Microwave Single-Crystal Si TFTs with f_{max} of 5.5 GHz," *Device Research Conference 2007 65th Annual*, 15–16 (2007).
12. L. Sun, G. Qin, J.-H. Seo, G. K. Celler, W. Zhou, and Z. Ma, "12-GHz Thin-Film Transistors on Transferrable Silicon Nanomembranes for High-Performance Flexible Electronics," *Small* **6**(22), 2553–2557 (2010).
13. G. Qin, H.-C. Yuan, G. K. Celler, W. Zhou, J. Ma, and Z. Ma, "RF model of flexible microwave single-crystalline silicon nanomembrane PIN diodes on plastic substrate," *Microelectron. J.* **42**(3), 509–514 (2011).

14. X. Xu, H. Subbaraman, A. Hosseini, C.-Y. Lin, D. Kwong, and R. T. Chen, "Stamp Printing of Silicon-Nanomembrane-Based Photonic Devices onto Flexible Substrates with a Suspended Configuration," *Opt. Lett.* **37**(6), 1020–1022 (2012).
 15. Z. Y. Dang, M. Motapothula, Y. S. Ow, T. Venkatesan, M. B. H. Breese, M. A. Rana, and A. Osman, "Fabrication of large-area ultra-thin single crystal silicon membranes," *Appl. Phys. Lett.* **99**(22), 223105 (2011).
 16. W. D. Zhou, Z. Q. Ma, H. J. Yang, Z. X. Qiang, G. X. Qin, H. Q. Pang, L. Chen, W. Q. Yang, S. Chuwongin, and D. Y. Zhao, "Flexible photonic-crystal Fano filters based on transferred semiconductor nanomembranes," *J. Phys. D Appl. Phys.* **42**(23), 234007 (2009).
 17. G. X. Qin, H. C. Yuan, G. K. Celler, W. D. Zhou, and Z. Q. Ma, "Flexible microwave PIN diodes and switches employing transferable single-crystal Si nanomembranes on plastic substrates," *J. Phys. D Appl. Phys.* **42**(23), 234006 (2009).
 18. M. J. Zablocki, A. Sharkawy, O. Ebil, and D. W. Prather, "Nanomembrane transfer process for intricate photonic device applications," *Opt. Lett.* **36**(1), 58–60 (2011).
 19. D. Taillaert, P. Bienstman, and R. Baets, "Compact efficient broadband grating coupler for silicon-on-insulator waveguides," *Opt. Lett.* **29**(23), 2749–2751 (2004).
 20. R. Halir, P. Cheben, S. Janz, D.-X. Xu, I. Molina-Fernández, and J. G. Wangüemert-Pérez, "Waveguide grating coupler with subwavelength microstructures," *Opt. Lett.* **34**(9), 1408–1410 (2009).
 21. R. Halir, P. Cheben, J. H. Schmid, R. Ma, D. Bedard, S. Janz, D. X. Xu, A. Densmore, J. Lapointe, and Í. Molina-Fernández, "Continuously apodized fiber-to-chip surface grating coupler with refractive index engineered subwavelength structure," *Opt. Lett.* **35**(19), 3243–3245 (2010).
 22. C. Xia and H. K. Tsang, "Nanoholes Grating Couplers for Coupling Between Silicon-on-Insulator Waveguides and Optical Fibers," *IEEE Photon. J.* **1**(3), 184–190 (2009).
 23. P. Yeh, A. Yariv, and C.-S. Hong, "Electromagnetic propagation in periodic stratified media. I. General theory," *J. Opt. Soc. Am.* **67**(4), 423 (1977).
 24. P. Bienstman and R. Baets, "Optical modelling of photonic crystals and VCSELs using eigenmode expansion and perfectly matched layers," *Opt. Quantum Electron.* **33**(4/5), 327–341 (2001).
-

1. Introduction

Progress in silicon photonics over the last 15 years, utilizing silicon-on-insulator (SOI) technology, has significantly moved conventional silicon VLSI to high speed, high bandwidth photonics with lower power consumption. Silicon based microelectronic, nano- and micro-photonic devices have the advantage of a compact structure with the potential for monolithic integration with optical-to-electrical on-chip conversion and detection.

There has been a recent growing interest to exploit the unique characteristics of semiconductor materials for the development of hybrid electronic and photonic devices on various material platforms [1–4]. Therefore, forming hybrid electronic/photonic devices on semiconductor nanomembranes have received tremendous attention over the last few years [5–15]. Of the various semiconductor nanomembranes (SiNM) studied, silicon nanomembranes are a natural choice for the development of high performance circuits and devices owing to a strong history of silicon photonics and microelectronics development.

Silicon nanomembranes are comprised of a very thin sheet of crystalline silicon that can be released from a silicon-on-insulator wafer [1]. Such membranes can be transferred and re-deposited on other rigid or flexible hosts such as glass, polyethylene terephthalate (PET), Kapton, etc using low temperature processes, thus providing hybrid integration and high performance devices. Similar to their SOI counterpart, silicon nanomembranes on other substrates are expected to exploit the same CMOS processing technologies that have resulted in widespread success of silicon photonics. Several interesting electronic and photonic devices have been demonstrated by employing SiNM on various substrates [2, 9–12]. Although the advances in SiNM based electronic devices have been significant, the development of SiNM based photonic devices has been limited. Most device demonstrations have relied on the surface-normal characteristics of photonic devices such as filters [16], photodetectors [17], and there are only a couple of demonstrations for in-plane SiNM photonic devices on other substrates [14, 18]. For successful in-plane SiNM photonic devices, one needs to overcome the challenges of intricate device development and light coupling on foreign substrates. The former has been addressed with novel SiNM transfer techniques [14, 18] to enable development of large aspect ratio SiNM photonic devices on foreign substrates. However, the latter still remains a challenge to overcome. Unlike conventional SOI based photonic devices, wherein facet preparation techniques have matured significantly, such techniques are improper for SiNM based photonic devices due to the soft polymer cladding

underneath the semiconductor membrane. Moreover, if the integration is performed on a flexible substrate, the problem becomes even more severe. Recently, utilizing a combination of photolithography and dicing, we demonstrated the first successful light coupling into stamp printed in-plane flexible silicon waveguides on a Kapton substrate [14] where an insertion loss of 25 dB was reported. However, the loss is still significantly high for successful deployment of such in-plane photonic devices. Conventional 1-D grating couplers that have led to high efficiency coupling into SOI based photonic devices can also be used. However, the additional processing steps required to fabricate conventional grating couplers make this approach less attractive.

To our knowledge, we report the first subwavelength grating coupler (SWG) to achieve low-loss coupling into in-plane SiNM-based photonic devices. Compared to conventional 1-D grating couplers, SWG couplers can be fabricated simultaneously along with photonic circuits and do not require any additional photolithography steps [19–22]. We demonstrate a coupling efficiency of 39.17% at a peak wavelength of 1555.56 nm, with 1dB and 3dB bandwidths of 29 nm and 57 nm, respectively. Utilization of such a coupler can rapidly push flexible photonics technology forward, thus opening avenues for a wide range of useful devices.

2. Design and Fabrication

The SWG consists of an array of periodic rectangular air holes with subwavelength dimensions formed in a 250 nm thick SiNM transferred onto a glass substrate with an SU-8 bottom cladding layer, as shown in Fig. 1.

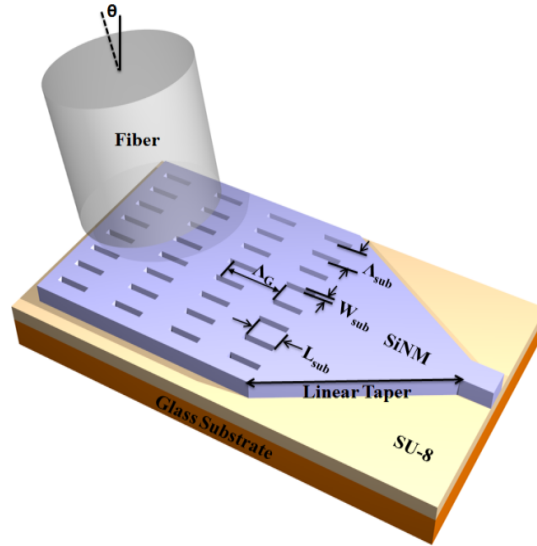


Fig. 1. Schematic illustration of the subwavelength grating (SWG) coupler on a SiNM transferred onto a glass substrate. L_{sub} , W_{sub} , Λ_{sub} , Λ_G , and θ denote the hole length, the hole width, the hole period, the grating period, and the angle of the fiber with respect to the surface normal, respectively.

Four grating parameters, namely, the trench length (L_{sub}), the hole width (W_{sub}), the hole period (Λ_{sub}), and the grating period (Λ_G) define the SWG. In order to simplify the calculations for an optimum design, an effective index approximation method, such as the Effective Material Theory (EMT) [20, 23], is utilized to approximate the subwavelength section as a uniform material with refractive index n_{sub} . An open source simulation package CAMFR, which is based on eigenmode expansion [24], is utilized to search for a best combination of grating period Λ_G and n_{sub} in order to obtain the highest power efficiency around 1550 nm. In our design, the filling factor of the grating is fixed at 50%. The calculated

optimum Λ_G and n_{sub} are $\Lambda_G = 0.690 \mu\text{m}$ and $n_{sub} = 2.45$, respectively, corresponding to $L_{sub} = 0.345 \mu\text{m}$, $W_{sub} = 0.090 \mu\text{m}$, and $\Lambda_{sub} = 0.390 \mu\text{m}$.

Fabrication is performed on a 2cm x 2cm 250nm thick SiNM transferred onto a 1mm thick glass substrate, with an 8.22 μm thick SU-8 bottom cladding layer, as shown in Fig. 2(a). The SiNM is transferred using a SOI bonding and handle wafer removal method similar to that described in [18]. In order to transfer the SiNM onto the 1mm thick glass substrate, a pre-cleaned 2 cm by 2 cm SOI chip (250 nm single crystal silicon layer, 3 μm buried oxide (BOX) layer and 500 μm handle wafer) and a 2.5 cm by 2.5 cm glass slide are spin coated with 5 μm thick SU-8 layer. After pre-baking, the SOI chip is brought into contact with the glass slide and pressure is applied. Next, the sample is heated to the glass transition temperature of SU-8 to enable reflow and removal of trapped air pockets. Then, ultra violet (UV) light is illuminated through the glass slide to cure SU-8. Post exposure baking is performed to complete cross linking. Following this, the 500 μm silicon handle is removed by polishing and deep silicon etching, with the 3 μm BOX layer serving as a stopping layer for the silicon etching process. The remaining 3 μm BOX is then selectively etched away using hydrofluoric acid, thus leaving a 250 nm silicon device layer with the SU-8 bottom cladding layer on the glass substrate. Twenty five periods of the designed SWG grating coupler are fabricated at the input and the output of an 8 mm long, 2.5 μm wide SiNM waveguide using electron beam lithography (JEOL JBX-6000). A pair of linear waveguide tapers, each with a length of 500 μm , is incorporated to bridge the 10 μm wide grating region to the waveguide. An SEM of the fabricated SiNM SWG coupler is shown in Fig. 2(b). A schematic of the fabricated structure is shown in the inset.

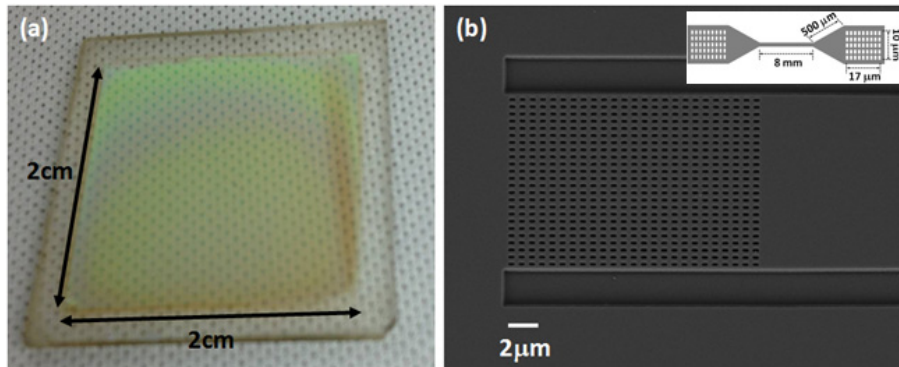


Fig. 2. (a) Optical microscope image of a 2cm x 2cm 250nm thick SiNM transferred onto a 1mm thick glass substrate. The thickness of the SU-8 bottom cladding layer is measured to be 8.22 μm , (b) Scanning electron microscope (SEM) image of the fabricated subwavelength grating coupler (SWG) on the transferred SiNM. A schematic of the fabricated structure is shown in the inset.

Since the SU-8 layer thickness cannot be controlled accurately using our custom-made bonding setup, the post fabrication measured SU-8 layer thickness of 8.22 μm is used to simulate the grating characteristics. Calculations are performed for TE polarization since that is the polarization of interest for several interesting photonic crystal waveguide and other active devices we are working on. The calculated back reflection (black curve), coupling efficiency to air (red curve), and coupling efficiency into a single mode fiber tilted at a 10 $^\circ$ angle with respect to the normal (blue curve) is shown as a function of wavelength in Fig. 3. At a wavelength of 1550nm, a peak upward power efficiency of 54%, corresponding to a 42% coupling efficiency into a single mode fiber, is achieved. Calculations for TE polarization are performed

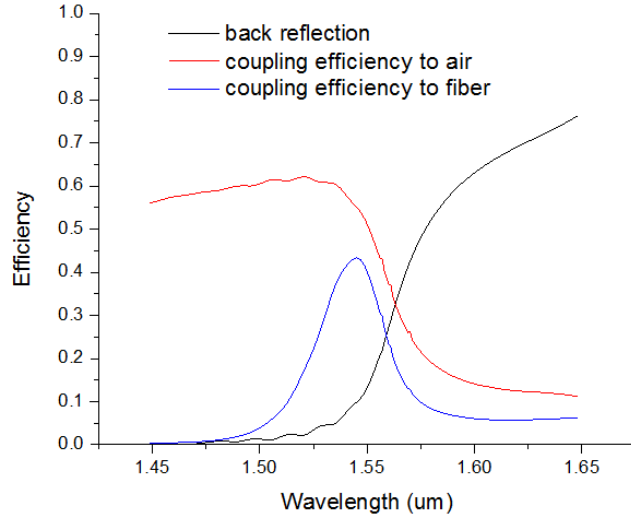


Fig. 3. Simulated back reflection (black), coupling efficiency to air (red) and coupling efficiency to a fiber positioned at 10° with respect to surface normal of the designed SWG coupler (blue) as a function of wavelength of operation. A peak fiber coupling efficiency of 42% is achieved at a wavelength of 1549nm. An SU-8 layer thickness of $8.22 \mu\text{m}$ is used in the simulation.

3. Device characterization

Our fabricated grating coupler is characterized by measuring the fiber-to-waveguide-to-fiber insertion loss. The input and output fibers are mounted on two 10° wedges, whose position with respect to the gratings can be controlled using two xyz stages. The input fiber is a polarization maintaining (PM) fiber whose polarization is controlled via a waveplate-based polarization controller (PC). The output fiber is a conventional single mode fiber with a core diameter of $9 \mu\text{m}$. The tilt angle can be adjusted from 0° to 20° . For this design, both the input and output fibers are tilted $\sim 9.4^\circ$ from normal incidence. TE polarized light from a broadband amplified spontaneous emission (ASE) source is coupled into the 8 mm long, $2.5 \mu\text{m}$ wide SiNM waveguide via the grating couplers. The transmission through the grating pair and the SiNM waveguide is measured on an optical spectrum analyzer (OSA). The coupling efficiency is extracted assuming equal coupling efficiencies for both gratings. Figure 4 shows the measured transmission spectrum for a single grating.

The peak efficiency is measured to be 39.17% (-4.07 dB) at 1555.56 nm. Measurements are also performed on a set of 5 pairs of grating couplers, and a maximum deviation in peak efficiency of -0.26 dB is obtained, thus showing a high uniformity in performance. The 1 dB and 3 dB bandwidths are measured to be 29 nm and 57 nm, respectively. The shift in the peak wavelength from the design value could possibly be due to fabrication errors which subsequently change n_{sub} from its designed value.

It should be noted, however, that the overall coupling efficiency is strongly affected by the thickness of the underlying SU-8 cladding layer. This is due to the fact that the constructive and destructive interference between the upward diffracted beam and the downward diffracted beam reflected upwards at the SU-8/glass interface is a periodic function of the cladding layer thickness. Due to the absence of a precise SiNM bonding tool, the SU-8 layer thickness cannot be controlled precisely. However, by utilizing a specialized bonding tool with a pressure monitoring system for the SiNM transfer process, the SU-8 layer thickness can be controlled accurately.

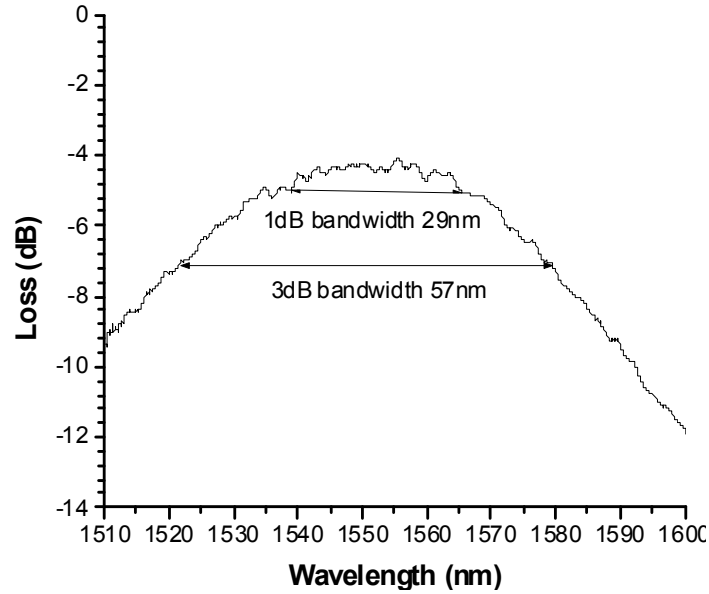


Fig. 4. Measured transmission spectrum of the grating coupler fabricated on SiNM on glass substrate. Peak efficiency of 39.17% (-4.07dB) is obtained at a wavelength of 1555.56nm. The 1 dB and 3 dB bandwidths are 29 nm and 57 nm, respectively.

Figure 5. is a simulation result showing the effect of changing the SU-8 layer thickness from $7\ \mu\text{m}$ to $9\ \mu\text{m}$ on the coupling efficiency to air. It can be seen that the efficiency fluctuates between 53% to 67% within $0.25\ \mu\text{m}$ of SU-8 layer thickness variation. Our measurement point is indicated as a red dot in the figure. Better control of the SU-8 layer thickness will further increase the efficiency. Nevertheless, the 'worst-case' scenario of 53% coupling efficiency to air is still better than other demonstrated coupling methods [14, 18].

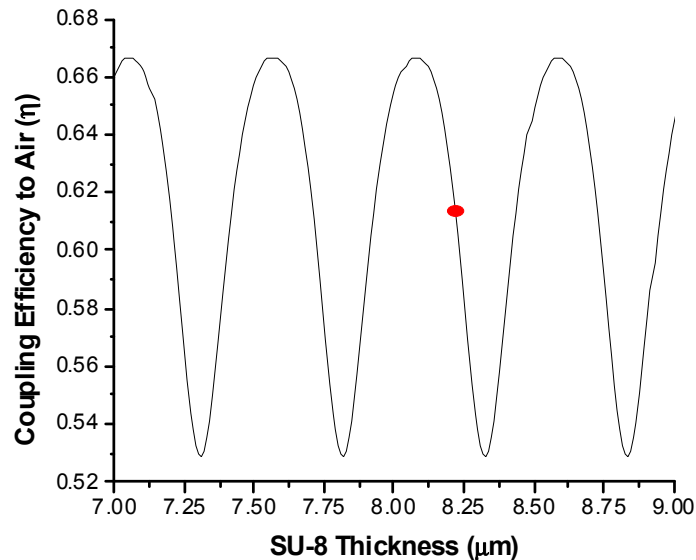


Fig. 5. Simulation showing the effect of SU-8 layer thickness variation from $7\ \mu\text{m}$ to $9\ \mu\text{m}$ on the coupling efficiency to air. A periodic efficiency fluctuation between 53% to 67% is produced. The red dot indicates our fabricated result.

4. Conclusion

In conclusion, we have developed a subwavelength grating (SWG) coupler consisting of an array of periodic trenches in SiNM transferred on glass substrate and demonstrated 39.17% (−4.07 dB) coupling efficiency into an 8 mm long, 2.5 μm long silicon waveguide. A coupling efficiency deviation of −0.26 dB is observed from a measurement of 5 grating pairs, indicating acceptable uniformity. The 1 dB and 3 dB bandwidths are measured to be 29 nm and 57 nm, respectively. Better coupling efficiency can be obtained by further improving the SiNM transfer process. This demonstration shows the first utilization of such efficient couplers for SiNM based in-plane photonic devices and opens vast possibilities for the development of high performance hybrid photonic components using nanomembrane technology.

Acknowledgments

This research was funded by Air Force Office of Scientific Research (AFOSR) STTR (Contract No. FA9550-11-C-0058 and FA9550-11-C-0014) and Multi-disciplinary University Research Initiative (MURI) program through the AFOSR (Contract No. FA 9550-08-1-0394) monitored by Dr. Gernot Pomrenke. Harish Subbaraman and Xiaochuan Xu contribute equally to this work.